Clay Minerals, (2009) **44**, 19–34

Evaluation of the structural model for ferrihydrite derived from real-space modelling of high-energy X-ray diffraction data

A. MANCEAU*

LGIT, Maison des Géosciences, CNRS and Université Joseph Fourier, 38041 Grenoble Cedex 9, France

(*Received 31 January 2008; revised 19 June 2008; Editor: Frédéric Villieras*)

ABSTRACT: A new structural model for ferrihydrite that challenges the standard ferrihydrite model established by X-ray diffraction and confirmed by neutron diffraction and single-crystal electron nanodiffraction was recently proposed by Michel *et al.* (2007a) from the simulation of the pair distribution function obtained by Fourier transformation of diffraction data measured at λ = 0.137 Å . The new ferrihydrite model is isostructural to akdalaite ($Al_{10}O_{14}(OH)_2$), a mineral having the Baker-Figgis δ-isomer of the Al_{13}-Keggin structure as its structural motif. The new model is unrealistic because: (1) it is completely periodic (i.e. defect-free); (2), it has 20% tetravalent octahedral iron ($^{VI}Fe^{4+}$), 20% divalent tetrahedral iron ($^{IV}Fe^{2+}$), and some $^{IV}Fe-O$ distances equal to or larger than the $^{VI}Fe^{3+}-O$ distances, thus violating Pauling's 2nd rule; (3) it does not describe X-ray diffraction and EXAFS spectroscopic data; and, (4) it is inconsistent with electron microscopy results and contradicts previous X-ray scattering studies.

KEYWORDS: ferrihydrite, feroxyhite, structure, PDF, XRD, EXAFS spectroscopy, bond valence.

Ferrihydrite is a widespread hydrous ferric oxyhydroxide in nature and is involved in many environmental, biological, and chemical processes. According to the standard model, ferrihydrite is a multiphase material which comprises three components, major defect-free crystallites (f-phase), minor defective crystallites (d-phase), and subordinate ultradisperse hematite (Drits *et al.*, 1993a). The f- and d-phases were confirmed by neutron diffraction (Jansen *et al.*, 2002), and all three components were observed by high-resolution transmission electron microscopy (HRTEM) (Drits *et al.*, 1995; Janney *et al.*, 2000, 2001) after they were first identified by X-ray diffraction (XRD). In addition, the three components were shown to comprise the core of the iron-storage protein, ferritin (Cowley *et al.*, 2000). Thus, the standard model describes all known occurrences of ferrihydrite, whether geological, biogenic, or synthetic.

The f-phase has a double-hexagonal ABACA layer stack and a random occupancy of 50% of the octahedral sites (Fig. 1a). The crystallographic structures derived from X-ray, neutron and electron diffraction are effectively the same, differing only slightly in site occupancies of the O and Fe sites and *z* coordinate of the Fe site (Table 1). The d-phase has even proportions of randomly alternating fragments with ABA and ACA stacking and a high degree of cation ordering in the oxygen and hydroxyl layers. It is structurally similar to feroxyhite (δ-FeOOH) (Drits *et al.*, 1993b). In feroxyhite, face-sharing octahedral pairs occupied by Fe atoms regularly alternate along the [001]

* E-mail: Alain.Manceau@obs.ujf-grenoble.fr
DOI: 10.1180/claymin.2009.044.1.19

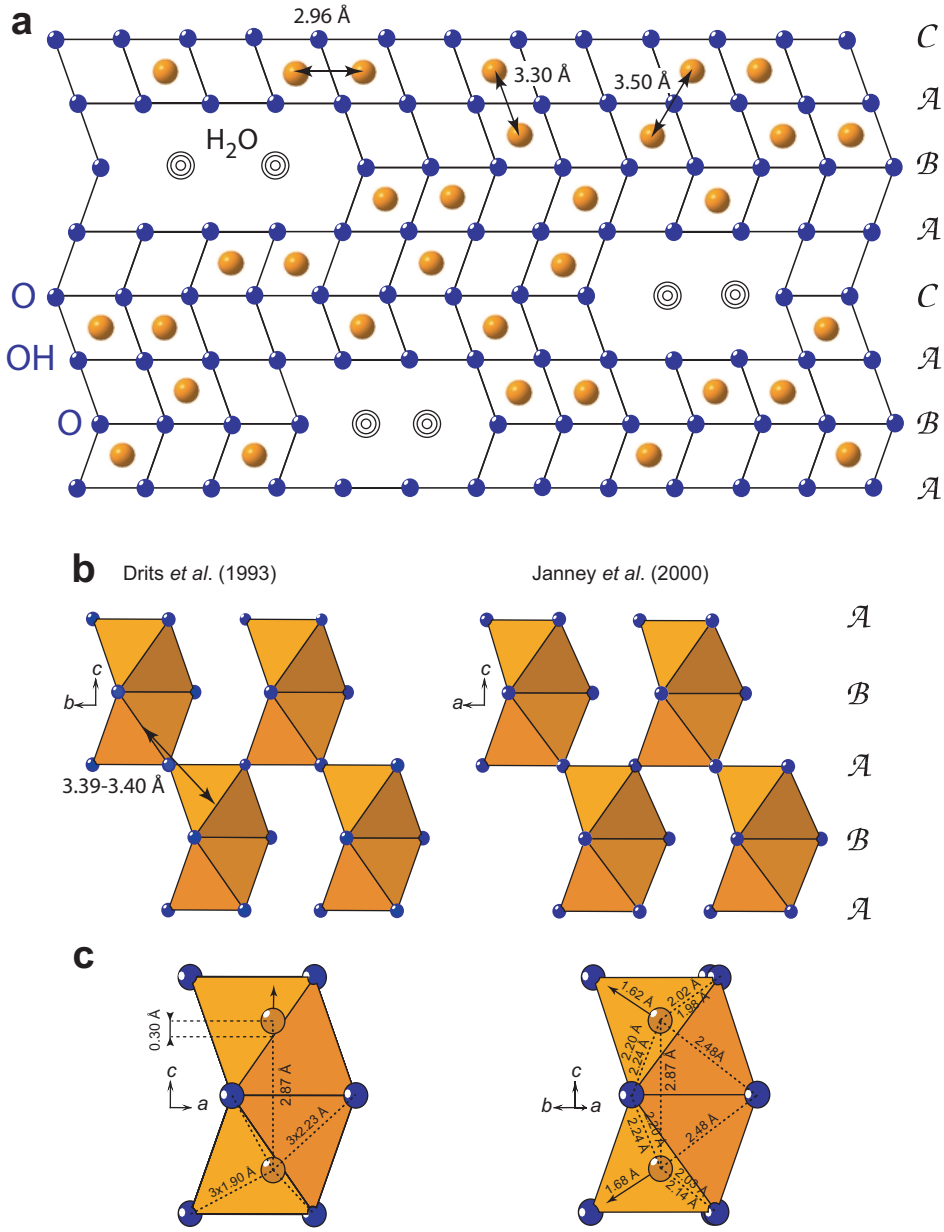

FIG. 1. (a) Projection of the defect-free component (f-phase) of ferrihydrite in the $(\bar{1}\bar{1}0)$ plane. (b) Polyhedral sketch of the connectivity of Fe octahedra in the feroxyhite-like domains (δ-FeOOH; Drits *et al.*, 1993b) and in the double-chain structures (Janney *et al.*, 2001) from the defective component (d-phase) of ferrihydrite. The atomic packing is AcBcA and 50% of the octahedral sites (c position) are occupied as in the two other FeOOH polymorphs, goethite (α-FeOOH) and akaganeite (β-FeOOH). (c) In feroxyhite, Fe atoms in face-sharing octahedra are off-centred in opposite directions along *c* as a consequence of cation repulsion, causing the Fe−O distances to split. The shift relative to the centre of the octahedron is 0.30 Å and the Fe-O distances equal 3×1.90 Å + 3×2.23 Å. In the double-chain model, Fe is displaced along a diagonal of the octahedron, resulting in abnormally short (1.62 Å) and long (2.48 Å) bond lengths. These distances are similar to those in the former feroxyhite model (1.78, 242 Å) by Patrat *et al.* (1983) revised by Drits *et al.* (1993b).

TABLE 1. Crystallographic data for defect-free ferrihydrite.

	Atom	*x*	*y*	*z*	Occupancy
Drits *et al.* (1993a)	Fe	1/3	2/3	0.15	0.5
a = 2.96 Å	O	0	0	0	1.0
c = 9.40 Å	O	2/3	1/3	1/4	0.85
Janney *et al.* (2001)	Fe	1/3	2/3	0.13	0.5
a = 3.00 Å	O	0	0	0	1.0
b = 9.40 Å	O	2/3	1/3	1/4	1.0
Jansen *et al.* (2002)	Fe	1/3	2/3	0.136	0.39
a = 2.955 Å	O	0	0	0	0.19
b = 9.37 Å	O	2/3	1/3	1/4	1.0

direction with vacant octahedral pairs, forming Fe-Fe-◇-◇-Fe-Fe chains (Fig. 1b). The 50% site occupancy of octahedral sites is maintained in the *ab* plane by shifting two consecutive chains up or down by two octahedra (Fe-◇-Fe-◇-Fe sequence in the [100] and [010] directions). This structure, derived from XRD, has exactly the same polyhedral connectivity as the double-chain structure for the d-phase derived from electron diffraction (Janney *et al.*, 2000), except that the interatomic distances differ in the two models (Fig. 1c). An important distinction between the f- and d-phases is that face-sharing octahedra occur only in the d-phase. This linkage is supported also by EXAFS spectroscopy (Combes *et al.*, 1990; Manceau & Drits, 1993). The third component in ferrihydrite is a combination of subordinate amounts of nanocrystalline phases, including hematite (α-Fe_2O_3) and a spinel-type phase (maghemite γ-Fe_2O_3 or magnetite Fe_3O_4), and highly defective material, in proportions that vary from sample to sample (Drits *et al.*, 1993a, 1995; Cowley *et al.*, 2000; Janney *et al.*, 2000, 2001; De Grave *et al.*, 2005).

Using X-ray absorption near-edge spectroscopy (XANES), Manceau *et al.* (1990) and Manceau and Gates (1997) ruled out the presence of tetrahedral Fe in the bulk and at the surface of ferrihydrite, in agreement with Mössbauer spectroscopy (Pankhurst & Pollard, 1992; De Grave *et al.*, 2005) and diffraction results. Also, bond-valence calculations suggested that Fe octahedra exposed at the surface of a ferrihydrite particle maintained a stable coordination by the dissociative sorption of one water layer and the physisorption of a second. The surface layer was considered to contain a mixture of singly (Fe_2-OH) and doubly (Fe-OH_2) protonated oxygens, depending on Fe coordination, the two protonation states inducing significant differences in octahedral relaxations and surface free energies. Water molecules in the adlayer would be oriented by hydrogen bonding with the hydroxylated surface. This model is consistent with surface diffraction (Catalano *et al.*, 2006; Tanwar *et al.*, 2007) and first-principles density function theory (DFT; Lo *et al.*, 2007) studies of defect-free metal oxides. Both types of results show that hydrated metal oxide surfaces contain stable polyhedral units in contact with water, display minor surface relaxations, and have two structured layers of water molecules above the hydroxylated layer. However, this comparison with perfect surfaces is not entirely compelling because the presence of numerous defects on heterogeneous surfaces may change water adsorption features significantly.

Recently, a single-phase model for ferrihydrite was proposed from the analysis of the real-space interatomic distances in the pair distribution function (PDF) derived from high-energy XRD (Fig. 2, Michel *et al.*, 2007a). The new model is isostructural with the mineral akdalaite ($Al_{10}O_{14}(OH)_2$) and its synthetic isomorph tohdite, a crystalline aluminium hydroxide compound consisting of a periodic assemblage of Baker-Figgis δ-Keggin isomers (i.e. Al_{13} entities) (Yamaguchi *et al.*, 1964; Yamaguchi & Okumiya, 1969; Hwang *et al.*, 2006). Three ferrihydrite samples with the same theoretical chemical composition ($Fe_{10}O_{14}(OH)_2$) and overall structure (i.e. space group) were refined by the PDF method, a six-line (Fhyd6), a three-line (Fhyd3), and a two-line (Fhyd2) ferrihydrite with domain dimensions (6, 3 and 2 nm) similar to those reported previously

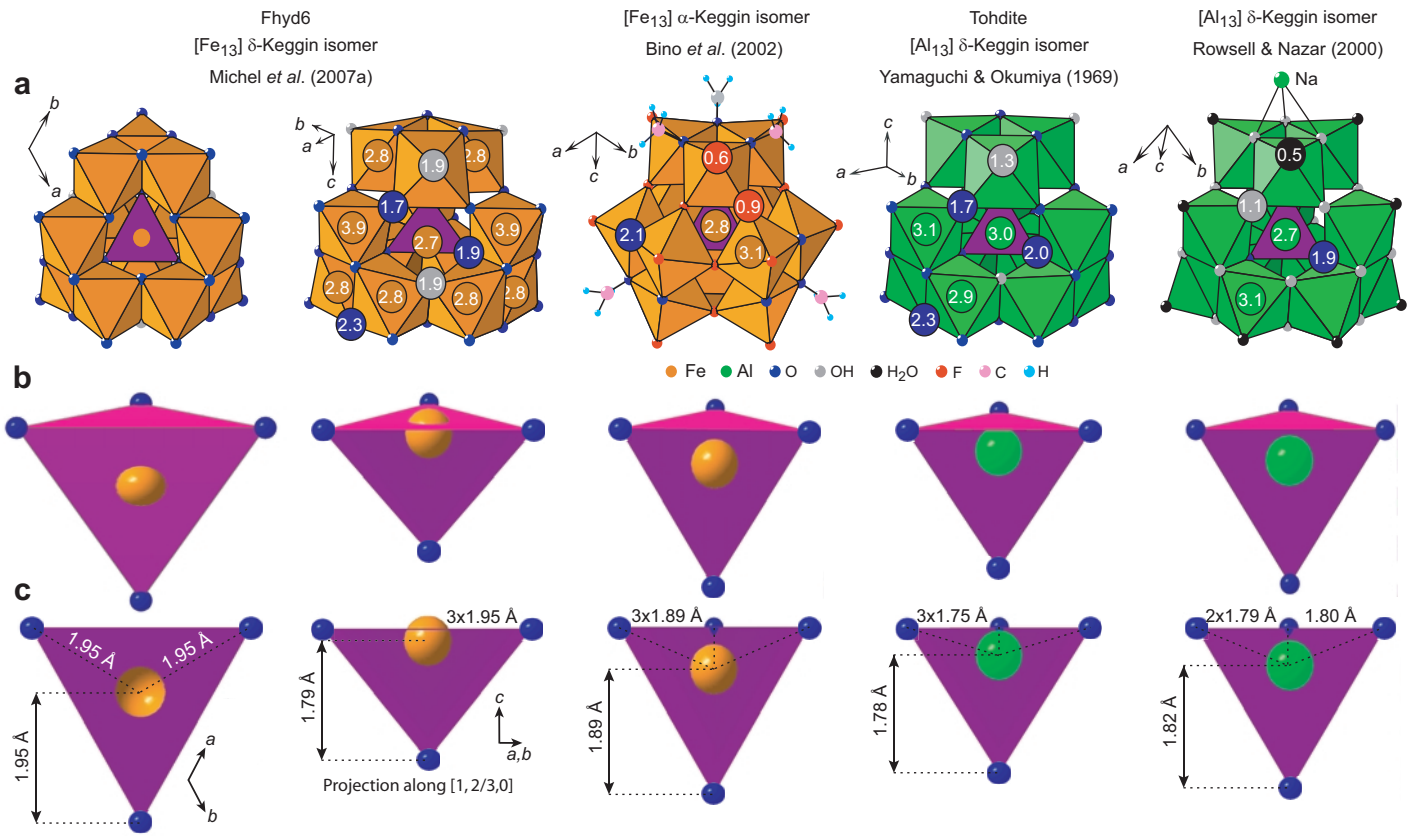

FIG. 2. Comparison of the [Fe_{13}] δ-Keggin structural motif proposed for ferrihydrite to chemical ([Fe_{13}] α-Keggin) and structural ([Al_{13}] δ-Keggin) analogues. On the left, the [Fe_{13}] δ-Keggin motif is viewed along the [001] direction as in the article by Michel *et al.* (2007a), and immediately to the right along the [1,2/3,0] direction. The [Fe_{13}] cluster appears symmetrical in the first projection, but extremely asymmetrical in the second, with some octahedra (^{VI}Fe) anomalously elongated and the tetrahedral Fe atom (^{IV}Fe) excessively off-centred. The numbers within the large circles are the valence charges at the Fe (light brown), Al (green), O (blue) and OH (grey) sites. The OH groups above and below, and the ^{VI}Fe atoms to the right and left, of ^{IV}Fe are highly oversaturated in ferrihydrite (1.9 and 3.9 v.u., instead of 1.0 and 3.0 v.u., respectively). Oxygens and hydroxyls were positioned as in tohdite ($Al_{10}O_{14}(OH)_2$; Yamaguchi & Okumiya, 1969), which is isostructural to akdalaite and the new ferrihydrite model. (b,c) View of the less symmetrical face of the Fe/Al tetrahedra (four sketches on the right) to show the unusual distortion of the FeO_4 δ-Keggin tetrahedron, which is not apparent when the structure is projected in the *ab* plane (leftmost sketch).

(Drits *et al.*, 1993a). The three samples were synthesized by the same protocol as that used in previous structural studies (Eggleton & Fitzpatrick, 1988; Drits *et al.*, 1993a; Manceau & Drits, 1993; Schwertmann *et al.*, 1999; Janney *et al.*, 2001). This protocol is a modification of the original recipe described by Towe and Bradley (1967), which involves the condensation and precipitation of Fe oligomers from a ferric salt solution. Since the new model is an assemblage of Fe_{13} entities, for chemical reasons the putative Fe_{13}-Keggin ions should have formed by hydrolysis in solution (Jolivet, 2000). So far, all attempts to precipitate Fe_{13} from aqueous solutions have been unsuccessful because this moiety has an extremely short life time (Bradley & Kydd, 1993). Therefore, the formation of ferrihydrite by polymerization of this unstable aqueous species is unlikely. In contrast, the Al_{13} moiety is metastable in solution and can be isolated in the solid state (Rowsell & Nazar, 2000), as observed in akdalaite and tohdite.

The new model also directly contradicts interpretations using the same PDF method on the same samples published by Michel *et al.* (2007b), only a few months before the Michel *et al.* (2007a) article. In the abstract of Michel *et al.* (2007b) it is stated: "... there are no significant differences in the underlying structures of these materials and [that] the differences in the diffraction patterns can be entirely interpreted by variations in the average size of the coherent scattering domains". In Michel *et al.* (2007a), the three 'materials' have acquired different unit-cell parameters and atomic coordinates, and thus quite different coordination chemistries, as

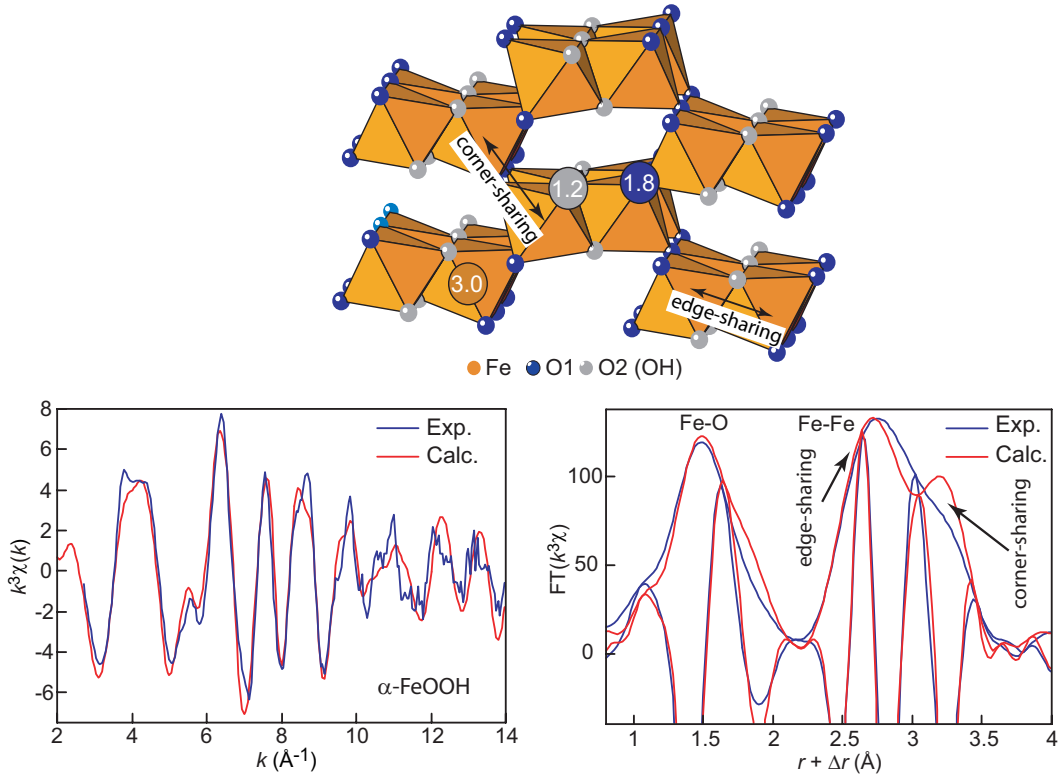

FIG. 3. Experimental and calculated EXAFS spectrum (left) and Fourier transform (right) for goethite (α-FeOOH). The theoretical spectrum was calculated *ab initio* using crystallographic data refined by the Rietveld method on the same sample used for EXAFS measurement (Hazemann *et al.*, 1991). This goethite has an incident bond-valence sum at the Fe site (3.0 v.u.) which is equal to the formal valence (+3, Table 2). The O1 site (oxygen atom) receives 1.8 v.u. from Fe atoms, and ~0.2 v.u. from the O1...H hydrogen bond (Brown, 1992; Hawthorne, 1994). The O2 site (OH group) receives 1.2 v.u. from Fe atoms, and ~0.8 v.u. from the O2−H bond. Bond-valence calculations were performed with R_0(Fe−O) = 1.759 Å and B = 0.37 Å (Brown & Altermatt, 1985).

shown below (i.e. to satisfy bond-valence rules two samples must have Fe^{4+} and one has Fe^{2+}).

The inconsistencies in structures proposed for the same samples in the two recent papers of Michel *et al.* (2007a,b) and the differences with structures reported in previous studies obtained with X-ray, neutron, and electron diffraction (Drits *et al.*, 1993a, 1995; Janney *et al.*, 2000, 2001; Jansen *et al.*, 2002), total X-ray scattering (Waychunas *et al.*, 1996), and extended X-ray absorption fine structure (EXAFS) spectroscopy (Manceau & Drits, 1993), prompt further evaluation of the new model.

EXPERIMENTS AND CALCULATIONS

Six-line (6Fh) and two-line (2Fh) ferrihydrites were synthesized by the same protocol used by Michel *et al.* (2007a,b). The XRD pattern of 6Fh was recorded on a D501 Siemens diffractometer using Co-$K\alpha$ radiation, a 0.02º2θ step interval and a 40 s counting time. Fe K-edge EXAFS spectra of 6Fh and 2Fh were recorded in transmission mode on the microfocus 10.3.2 beamline at the Advanced Light Source, Berkeley (USA). The technical characteristics of this beamline are described elsewhere (Manceau *et al.*, 2002; Marcus *et al.*, 2004). Six spectra from distinct spots homogenous at the scale of the beam size (16×7 μm^2) and having an absorption edge jump between 0.7 and 1.0 absorption lengths were recorded, and then averaged to improve the signal-to-noise ratio. Recording independent μ-EXAFS spectra from different parts of the same sample, and verifying that they are all statistically invariant before summation, helps minimize distortions to the data due to non-uniformity in sample thickness at smaller scale, i.e. 'hole effects' (Stern & Kim, 1981).

The EXAFS spectra for the Fhyd6 and Fhyd2 models were calculated *ab initio* with the FEFF 7.01 code (Ankudinov *et al.*, 1998) using crystallographic data reported in Tables S1 and S2 of Michel *et al.* (2007a). The spectrum for goethite was used as a reference to: (1) verify the correctness of the mean-free path of the electron (λ) and the amplitude and phase shift functions calculated *ab initio*; (2) calibrate the many-body amplitude-reduction factor (S_0^2) and the energy threshold (ΔE); and (3) optimize the mean-square displacement of bond length parameter (σ). Good agreement between experimental and calculated spectra for goethite was obtained by setting S_0^2 to 0.8, ΔE to 0.0 eV, σ = 0.052 Å for the short distance Fe–O pair, σ = 0.062 Å for the edge-sharing and corner-sharing Fe-Fe pairs, and σ = 0.108 Å for all greater-distance atomic pairs and three- and four-legged multiple-scattering paths (Fig. 3, Table 2). All these values are consistent with previous studies (Manceau *et al.*, 1998). Still better spectral agreement could be obtained by taking different disorder parameters for distant shells and single and multiple scattering paths, but this improvement does not necessarily indicate a better description of the data because of the increase in the number of variable parameters. The optimum S_0^2 and ΔE values determined for goethite were transferred to simulations of ferrihydrite spectra, taking into account the multiplicity of the Fe1, Fe2 and Fe3 sites.

RESULTS AND DISCUSSION

X-ray diffraction

The experimental XRD pattern for 6Fh (Fig. 4) resembles the experimental Fhyd6 pattern published

TABLE 2. Bond lengths and bond-valence table for goethite after the structural refinement of Hazemann *et al.* (1991).

Goethite	*d* (Å)	Fe (4c)	Sum	Type
O1(4c)	1.90	0.603, 0.584x2	1.77	O
O2 (4c)	2.10	0.407, 0.395x2	1.20	OH
Sum		2.97		

The bond-valence distribution of the proton is ~0.80 v.u. to the closer O2 atom and ~0.20 v.u. to the further O1 atom, as usually observed in ionic structures (Brown, 1976, 1992; Hawthorne, 1994).

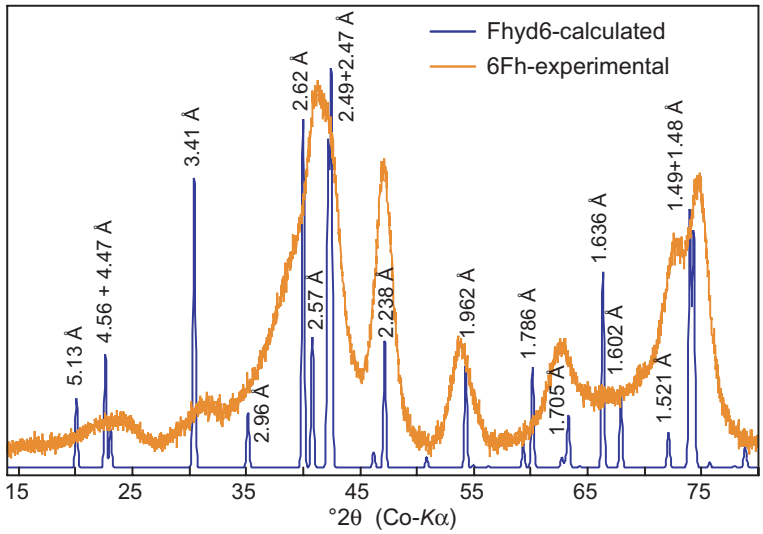

FIG. 4. The XRD pattern of the new model contains extra peaks not observed in the data, and the peaks which are common to the model and the data do not have the same relative heights or widths mainly because the new model is single phase and fully periodic. A similar discrepancy between the data and a defect-free single phase was reported in figure 7 of the article by Janney *et al.* (2001).

by Michel *et al.* (2007b), except for the relative intensities of the reflections at ~2.24 Å and ~1.71 Å for Fhyd6, which are weaker and slightly stronger, respectively, than usual (Eggleton & Fitzpatrick, 1988; Drits *et al.*, 1993a; Schwertmann *et al.*, 1999). These differences in X-ray intensity may result from feroxyhite (δ-FeOOH) impurity in Fhyd6, as reported in other specimens (Drits *et al.*, 1993a), or an excess of the d-phase.

The XRD trace calculated for the Fhyd6 structural model derived from the simulation of PDF data (Michel *et al.*, 2007a) has intense peaks at 3.4 Å and 1.64 Å that are absent from all experimental patterns of six-line ferrihydrite, including Fhyd6 (Michel *et al.*, 2007b) and 6Fh (Fig. 4). Also, experimental patterns have a peak at 1.73 Å and a shoulder at 1.51 Å that are not reproduced by the new model. The mismatch between data and model is even greater for Fhyd3 and Fhyd2 because three- and two-line ferrihydrites have a greater density of defects than six-line ferrihydrite (smaller domain size), and the new model is fully periodic. It is known that highly defective structures cannot be described with a periodic defect-free model, which is the reason why the new model fails to reproduce XRD data. However, Michel *et al.* (2007a) preferred their new model over the standard model (Drits *et al.*, 1993a) on the grounds that it provided a better match to the pair distribution functions, $G(r)$, obtained by Fourier transformation of the high-energy diffraction data. This interpretation is misleading for two reasons.

First, the $G(r)$ functions were calculated with the assumption that ferrihydrite is a single phase, which previously had been disproven (Drits *et al.*, 1995; Janney *et al.*, 2001; Jansen *et al.*, 2002). Furthermore, none of the three components from the standard model reproduces the XRD data separately (Drits *et al.*, 1993a). Therefore, by showing (Figure S1 in Michel *et al.*, 2007a) that neither the f-phase nor the d-phase alone reproduce the $G(r)$ data, Michel *et al.* (2007a) simply have agreed with previous XRD and modelling results and did not provide new evidence to rebut the standard model. To test whether the full standard model can explain the $G(r)$ data, the mathematical formalism that describes the Markovian probability of occupancy of Fe and O atoms in the f- and d-phases should be included in the calculation (Drits *et al.*, 1993a). Unfortunately, this is not currently possible because existing pair distribution function (PDF) programs require defect-free crystals or isolated molecular units of identical type (Waychunas *et al.*, 1996). This limitation can be circumvented by calculating in reciprocal space the

structure function $S(Q)$ for the three-component mixture and Fourier transforming $S(Q)$ to obtain $G(r)$.

Second, close examination of the theoretical PDFs calculated by Michel *et al.* (2007a) for the f- and d-phases shows an obvious error in the calculations (Fig. 5). In the standard model, the two primary components contain many octahedral linkages with Fe−Fe distances of 3.30 to 3.50 Å that average to ~3.40 Å (Fig. 1). This intense correlation is absent from the PDF calculations and instead there is a strong peak at ~3.6 Å. In fact, the two theoretical PDFs, shown in Fig. 5, were calculated using crystallographic parameters derived from neutron diffraction data (Jansen *et al.*, 2002), as reported in entries #97586 and #97587 of the Inorganic Crystal Structure Database (ICSD), instead of those derived from X-ray data, as reported in the original article by Drits *et al.* (1993a) (F.M. Michel, pers. comm.). As stated by the authors of the neutron study: 'the scattering conditions were extraordinarily unfavourable due to (i) the high incoherent background occurring from the large amount of hydrogen in the compound and (ii) the large peak widths caused by the nanocrystalline nature of the ferrihydrite', and thus, 'the refinement calculations were rather poor'. The lesser quality of the neutron refinement is demonstrated, for example, by the inconsistency of the Fe and O site occupancies obtained with neutron diffraction *vs*. those derived from X-ray and electron diffraction (Table 1).

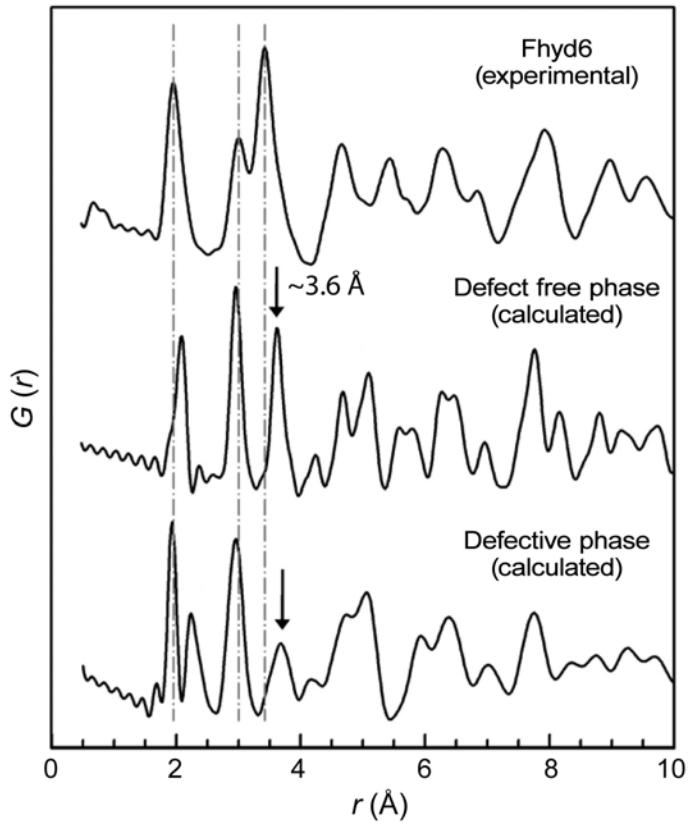

FIG. 5. Experimental pair distribution function (PDF) for Fhyd6 compared to PDFs for the defective and defect-free phases of ferrihydrite, as calculated by Michel *et al.* (2007a). Vertical lines highlight positions of the first three main correlations in Fhyd6 at ~2.0 (Fe−O,OH bond length), ~3.0 (mostly Fe−Fe pairs across edges), and ~3.4 Å (mostly Fe−Fe pairs across corners with some contribution from long edge-sharing distances). There is an apparent error in the calculations because in the standard model from Drits *et al*. (1993a) both the f- and d-phases contain intense Fe−Fe correlations at ~3.4 Å and no (f-phase), or weak (d-phase), correlation at ~3.6 Å (arrows).

TABLE 3. Bond lengths and bond-valence table for Fhyd6. The values in bold are unrealistic.

Fhyd6	— ^{VI}Fe1 (6c) —		— ^{VI}Fe2 (2b) —		– ^{IV}Fe3 (2b) –		Sum	Type
	d (Å)	BV	*d* (Å)	BV	*d* (Å)	BV		
O1 (2a)	1.93	$0.625 \times 3\rightarrow$					**1.87**	OH
O2 (2b)	2.04	$0.467 \times 3\rightarrow$			1.79	0.920	2.32	O
O3 (6c)	2.01×2	0.505×2	1.87×3	$0.733 \times 3\downarrow$			1.74	O
O4 (6c)	2.14×2	0.357×2	1.96×3	$0.575 \times 3\downarrow$	1.95×3	$0.592 \times 3\downarrow$	1.88	O
Mean/sum	2.05 $\sigma = 0.08$	2.82	**1.92** $\sigma = 0.05$	**3.92**	1.91 $\sigma = 0.08$	2.70		

The arrows in the bond-valence columns (BV) indicate the sum (vertical *vs*. horizontal) to which the multiplicative factor is applied. The proton is assumed to be held by O1, as in tohdite. Since the O–H bond typically contributes a bond valence of ~0.8 v.u. to the O atom, the incident bond-valence at the O1 site from the three Fe1 atoms should sum to ~1.2 v.u. The bond-valence sum of the Fe sites should be close to 3.0, as in goethite (Table 2). The σ value for all Fe–O distances in the unit cell is 0.09 Å.

EXAFS spectroscopy

The new ferrihydrite model also has significant shortcomings in reproducing EXAFS data (Fig. 6). Spectra calculated for the Fhyd6 and Fhyd2 models do not reproduce the experimental wave frequency over most of the wavevector (*k*) range (i.e. interatomic distances in real space), nor the fine structure of the EXAFS oscillations (i.e. polyhedral connectivity) (Fig. 6a). The Fhyd6 and Fhyd2 spectra are shifted in frequency because the two model structures do not have the same unit-cell dimensions and atomic coordinates (i.e. interatomic distances), and to a lesser extent site occupancies (number of Fe–O and Fe–Fe pairs). The calculated Fhyd2 spectrum has a greater amplitude than the Fhyd6 spectrum, which is unexpected because two-line ferrihydrite is less crystallized (i.e. has a smaller domain size) than six-line ferrihydrite.

Radial structure functions derived from EXAFS spectra show that the Fe–O and Fe–Fe distances in the model differ from observed values, and that the Fe–O pair has a greater amplitude in the least crystalline Fhyd2 sample, as observed before from the EXAFS oscillations (Fig. 6b). The anomalous amplitude of the Fe–O pair in poorly crystallized Fhyd2 results from the small standard deviation of the Fe–O distances ($\sigma = 0.06$ Å) in the structural model; the distribution of the Fe–O bond lengths being unrealistically broader in the model for the more crystalline Fhyd6 ($\sigma = 0.09$ Å, Tables 3, 4, and 5). Similarly to the Fe–O distances, the interval of variation for the Fe–Fe distances in the new model is also problematic. The mean Fe–Fe distances across octahedral edges are the same in Fhyd6 and Fhyd2 (3.03–3.04 Å), but the standard deviation is 0.12 Å in the model representing the more crystalline material and

TABLE 4. Bond length and bond-valence table for Fhyd3. The values in bold are unrealistic.

Fhyd3	— ^{VI}Fe1 (6c) —		— ^{VI}Fe2 (2b) —		– ^{IV}Fe3 (2b) –		Sum	Type
	d (Å)	BV	*d* (Å)	BV	*d* (Å)	BV		
O1 (2a)	1.92	$0.642 \times 3\rightarrow$					**1.93**	OH
O2 (2b)	2.06	$0.439 \times 3\rightarrow$			1.77	0.963	2.28	O
O3 (6c)	2.00×2	0.521×2	1.90×3	$0.691 \times 3\downarrow$			1.73	O
O4 (6c)	2.14×2	0.356×2	1.95×3	$0.595 \times 3\downarrow$	1.99×3	$0.534 \times 3\downarrow$	1.84	O
Mean/sum	2.04 $\sigma = 0.08$	2.83	**1.92** $\sigma = 0.03$	**3.86**	1.94 $\sigma = 0.11$	2.56		

The σ value for all Fe–O distances in the unit cell is 0.09 Å.

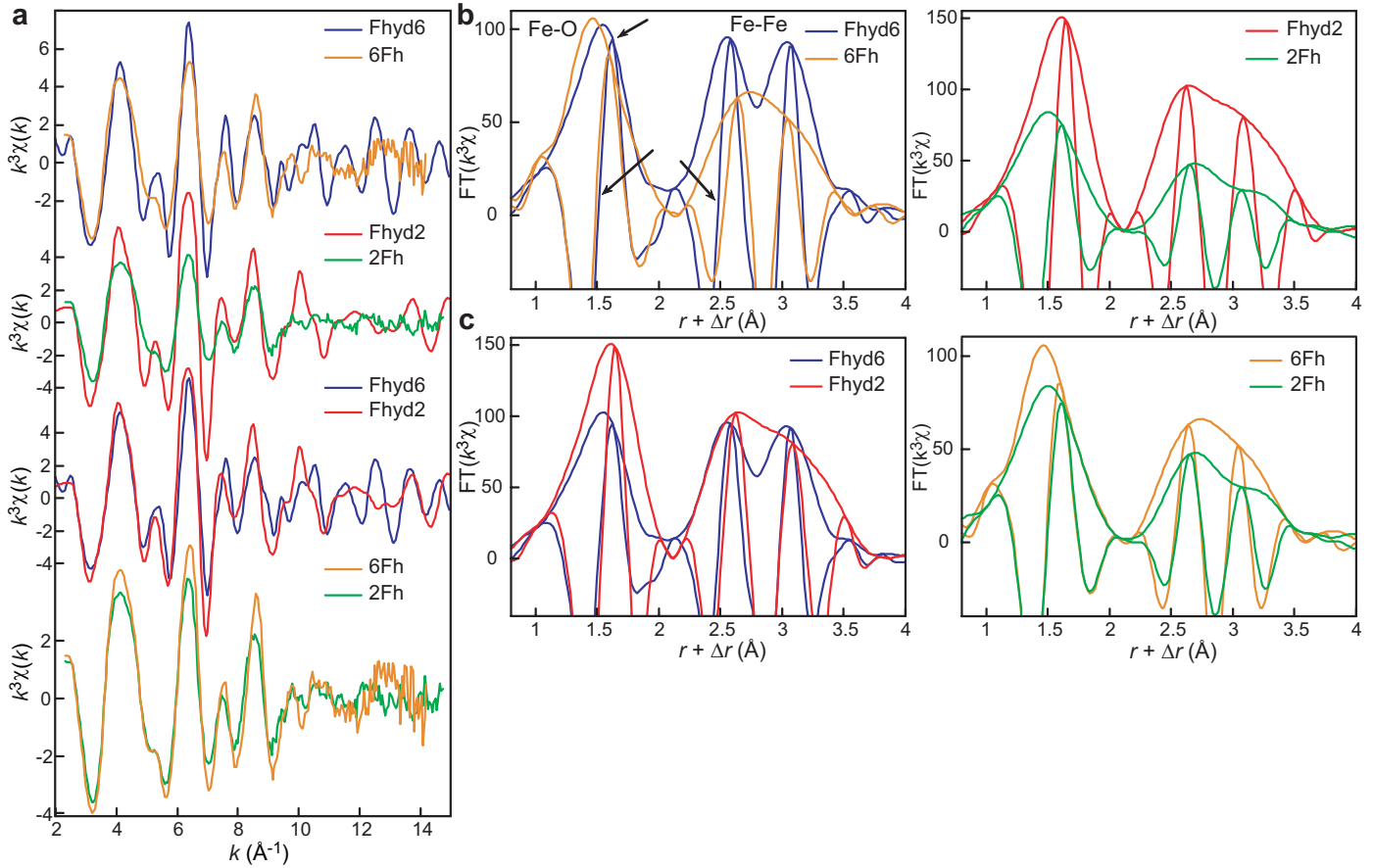

FIG. 6. EXAFS data for the new six-line (Fhyd6) and two-line (Fhyd2) ferrihydrite models compared to experimental data (6Fh, 2Fh). (a) EXAFS spectra. (b,c) Fourier transforms (modulus plus imaginary part). Two-line ferrihydrite (2Fh) has a smaller EXAFS amplitude than six-line (6Fh) because it is less crystalline, but the same wave frequency and shape because Fe atoms have similar bonding environments in the two types of ferrihydrites (Drits *et al.*, 1993a; Manceau & Drits, 1993). This experimental similarity is inconsistent with the distinct unit-cell dimensions and atomic coordinates for Fhyd6, Fhyd3 and Fhyd2 from the new model (tables S1 and S2 in Michel *et al.*, 2007a).

TABLE 5. Bond length and bond-valence table for Fhyd2. The values in bold are unrealistic.

Fhyd2	— ^{VI}Fe1 (6c) —		— ^{VI}Fe2 (2b) —		– ^{IV}Fe3 (2b) –		Sum	Type
	d (Å)	BV	*d* (Å)	BV	*d* (Å)	BV		
O1 (2a)	2.05	$0.453 \times 3\rightarrow$					1.36	OH
O2 (2b)	1.92	$0.649 \times 3\rightarrow$			1.96	0.582	**2.53**	O
O3 (6c)	2.04×2	0.473×2	1.88×3	$0.713 \times 3\downarrow$			1.66	O
O4 (6c)	1.98×2	0.550×2	2.08×3	$0.418 \times 3\downarrow$	2.02×3	$0.495 \times 3\downarrow$	2.01	O
Mean/sum	2.00 $\sigma = 0.05$	3.15	1.98 $\sigma = 0.11$	3.39	**2.00** $\sigma = 0.03$	**2.07**		

The σ value for all Fe−O distances in the unit cell is 0.06 Å.

0.08 Å in the model representing the less crystalline material. Some Fe−Fe distances are unusually short or long for a ferric oxyhydroxide. For example, Fhyd6 has an Fe1−Fe1 distance (2.91 Å) that is typical of a face-sharing linkage (Blake *et al.*, 1966), and not the expected edge-sharing linkage (Manceau & Combes, 1988; Manceau & Drits, 1993). These oddities explain why Fhyd2 and Fhyd6 have their imaginary parts shifted in the [2.2−3.5 Å] $r+\Delta r$ interval, in contrast to 2Fh and 6Fh (Fig. 6c).

Bond-valence calculations

Model compounds. Bond-valence calculations (Brown & Altermatt, 1985) were performed first on known structures containing [Fe_{13}] or [Al_{13}] tridecamer units to verify the validity of this approach for determining the distribution of effective charges among cations and anions in the new ferrihydrite model. Three model compounds were examined (Fig. 2): an [Fe_{13}] cluster ($Fe_{13}O_4F_{24}(OMe)_{12}$; Bino *et al.*, 2002) and two [Al_{13}] clusters, tohdite ($Al_{10}O_{14}(OH)_2$; Yamaguchi & Okumiya, 1969) and the Na-δ-[Al_{13}] cluster ($Al_{13}O_4(OH)_{24}(H_2O)_{12}(SO_4)_4{\cdot}19H_2O$; Rowsell & Nazar, 2000). These structures provide context for the plausibility of the [Fe_{13}] core in ferrihydrite, yet none were discussed by Michel *et al.* (2007a).

The $Fe_{13}O_4F_{24}(OMe)_{12}$ cluster was synthesized by reacting $FeF_3{\cdot}3H_2O$ and pyridine in hot methanol under anoxic conditions. It adopts the structure of the α-isomer, rather than the δ- or ε-isomer structure of the Al_{13} polyoxoaluminium cations. This cluster has an ideal α-Keggin structure with 12 surrounding iron atoms and a central tetrahedral $^{IV}FeO_4$ core. It is highly symmetrical ($F\bar{4}3m$ space group), with a central tetrahehron having full *Td* symmetry (Fig. 2). Thus, ^{IV}Fe resides at the centre of the tetrahedron, i.e. at a distance one fourth of the height from any opposite base ($h = 1/4H$). All cations and anions are saturated to within 0.2 v.u., and even to 0.1 v.u. if one excludes the tetrahedral cation which is too small for an ideal fit (Bradley *et al.*, 1992; Rowsell & Nazar, 2000) (Table 6). In comparison, ^{IV}Fe in the Fhyd6 model is at $h = 0.095$ from one tetrahedral face, and in projection on this face at

TABLE 6. Bond-valence table for the [Fe_{13}] α-Keggin cluster (Bino *et al*., 2002).

	^{IV}Fe1 (4b)	^{VI}Fe2 (48h)	C1 (48h)	Sum	Type
O1 (16e)	$0.708 \times 4\downarrow$	$0.403 \times 3\rightarrow$		1.92	O
O2 (48h)		0.568×2	0.925	2.06	O
F1 (48h)		0.444×2		0.89	F
F2 (48h)		0.642		0.64*	F
Sum	2.83	3.07			

* Charge balanced with two H bonds

~1/3 from the three oxygen vertices, that is close to the centre of gravity of the tetrahedral face (Fig. 2). This equilateral face is parallel to the *ab* plane. This topology is unrealistic for a tetrahedron. More generally, the three [Fe_{13}] ferrihydrite clusters proposed by Michel *et al.* (2007a) (Fhyd6, Fhyd3, Fhyd2) are severely distorted compared to the $Fe_{13}O_4F_{24}(OMe)_{12}$ cluster, and several Fe and O atoms have missing or excess valence charge (Tables 3–5).

According to Michel *et al.* (2007a), tohdite is also isostructural with Fhyd6, Fhyd3 and Fhyd2 because it has the same structure and composition as akdalaite. Therefore, the distribution of charges should be similar in tohdite and ferrihydrite. Tohdite has two octahedral Al^{3+} (Al1, Al2) and one tetrahedral Al^{3+} (Al3) in the asymmetric unit (Table 7). The three Al atoms are saturated to within 0.15 v.u., one oxygen (O2) has its charge well balanced, while two others have a charge excess or deficit of 0.3 v.u. With a bond-valence sum of 1.3 v.u., and a multiplicity (2a position) equal to the stoichiometry of OH groups in the chemical formula (i.e. 2), the O1 site is presumably an hydroxo group (Li *et al.*, 1998) (Table 7). Thus, the proton ideally donates 0.7 positive charge to O1. The equivalent O1 position in the Fhyd6 and Fhyd3 models is too oversaturated (1.9 v.u.) to hold a proton (Tables 3, 4). Therefore, the position of protons in the new ferrihydrite model is indeterminate.

The structure of the Na-δ-[Al_{13}] cluster has been refined on a single crystal (Rowsell & Nazar, 2000), and thus may be an even better comparison to ferrihydrite than tohdite, for which the structure has been determined on X-ray powder data (Yamaguchi & Okumiya, 1969). The four ^{IV}Al–O distances are equal to within 0.03 Å and ^{IV}Al is close to the centre of the tetrahedron ($h \approx 0.23H$, Fig. 2). As is usually the case in [Al_{13}] clusters, ^{IV}Al is too small for the tetrahedral cage, and consequently is slightly undersaturated (2.7 v.u.). The bond-valence sums for the O, OH and H_2O ligands, averaged over all positions, show saturation within 0.1 v.u (Table 8), which contrasts strongly with the bond-valence sums for anions in Fhyd6, Fhyd3, and Fhyd2. Thus, this analysis shows that the bond-valence sum method predicts the correct oxidation state of the metal centres in all known analogues to the new ferrihydrite model.

New ferrihydrite model. The ^{VI}Fe2 site has a large excess of valence (+0.9 v.u.) in Fhyd6 and Fhyd3, and the ^{IV}Fe3 site has a large deficit of valence (−0.9 v.u.) in Fhyd2 (Tables 3, 4, and 5). Therefore, 20% of the Fe must be tetravalent and octahedral ($^{VI}Fe^{4+}$) in Fhyd6 and Fhyd3, and divalent and tetrahedral ($^{IV}Fe^{2+}$) in Fhyd2 to attain reasonable bond valences. However, these distributions of charge and site occupancies are unrealistic and together undercut the validity of the new ferrihydrite model. Also, Fe^{4+} cannot be stabilized in the structure of a ferric oxyhydroxide synthesized under ambient conditions, and no minerals or materials at the Earth's surface have ever been shown to contain tetravalent iron. Similarly, $^{IV}Fe^{2+}$ has never been described in this type of compound. Also, with a bond-valence sum of 1.9 v.u., the OH group (O1 site) is anomalously oversaturated in Fhyd6 and Fhyd3 (Hawthorne, 1994). Substituting the OH group by a water molecule in the structure does not alleviate the problem because the incident bond-valence at the O1 site from the three coordinating ^{VI}Fe1 cations should be close to 0.4 v.u. instead of ~1.2 v.u. for a hydroxyl group. One should note in passing that the

TABLE 7. Bond-valence table for the [Al_{13}] δ-Keggin cluster, tohdite ($Al_{10}O_{14}(OH)_2$) (Yamaguchi & Okumiya, 1969).

	^{VI}Al1 (6c)	^{VI}Al2 (2b)	^{IV}Al3 (2b)	Sum	Type
O1 (2a)	$0.443 \times 3\rightarrow$			1.33	OH*
O2 (6c)	0.374×2	$0.454 \times 3\downarrow$	$0.761 \times 3\downarrow$	1.96	O
O3 (6c)	0.567×2	$0.575 \times 3\downarrow$		1.71	O
O4 (2b)	$0.540 \times 3\rightarrow$		0.713	2.33	O
Sum	2.86	3.09	3.00		

* Assignation based on structural formula and crystallographic multiplicity.
In contrast to Fhyd6, Fhyd3 and Fhyd2, all cations are saturated within 0.15 v.u and oxygens within 0.3 v.u.

TABLE 8. Bond-valence table for the [Al_{13}] δ-Keggin cluster, Na-δ-[$Al_{13}O_4(OH)_{24}(H_2O)_{12}$][$SO_4$]$_4$·19$H_2O$ (Bino *et al*., 2002).

	^{IV}Al1	^{VI}Al2	^{VI}Al3	^{VI}Al4	^{VI}Al5	^{VI}Al6	^{VI}Al7	^{VI}Al8	^{VI}Al9	^{VI}Al10	^{VI}Al11	^{VI}Al12	^{VI}Al13	Na	Sum	Type
O1	0.672	0.423	0.371	0.375											1.84	O
O2	0.687				0.339	0.398	0.448								1.87	O
O3	0.691							0.353	0.393	0.429					1.87	O
O4	0.633										0.429	0.421	0.435		1.92	O
O5		0.536										0.549			1.09	OH
O6		0.546											0.562		1.11	OH
O7		0.555	0.584												1.14	OH
O8		0.476		0.537											1.01	OH
O9			0.556			0.549									1.11	OH
O10			0.575			0.598									1.17	OH
O11			0.531	0.572											1.10	OH
O12				0.586					0.582						1.17	OH
O13				0.533					0.519						1.05	OH
O14					0.558		0.541								1.10	OH
O15					0.555	0.549									1.10	OH
O16					0.586			0.576							1.16	OH
O17					0.602			0.600							1.20	OH
O18						0.550	0.507								1.06	OH
O19							0.559				0.575				1.13	OH
O20							0.513						0.541		1.05	OH
O21								0.618	0.607						1.22	OH
O22								0.573		0.576					1.15	OH
O23									0.527	0.451					0.98	OH
O24										0.556	0.587				1.14	OH
O25										0.575		0.572			1.15	OH
O26											0.509	0.521		0.234	1.26	OH
O27											0.516		0.521	0.209	1.25	OH
O28												0.568	0.501	0.113	1.18	OH
O29		0.487													0.49	H_2O
O30			0.490												0.49	H_2O
O31				0.465											0.47	H_2O
O32					0.499										0.50	H_2O
O33						0.440									0.44	H_2O
O34							0.485								0.49	H_2O
O35								0.448							0.45	H_2O
O36									0.469						0.47	H_2O
O37										0.507					0.51	H_2O
O38											0.502				0.50	H_2O
O39												0.507			0.51	H_2O
O40													0.507		0.51	H_2O
O41														0.216	0.22	H_2O
O42														0.149	0.15	H_2O
O43														0.282	0.28	H_2O
Sum	2.68	3.02	3.11	3.07	3.14	3.08	3.05	3.17	3.10	3.09	3.12	3.14	3.07	1.20		

The bond valences reported in Fig. 2 are average values.

new model does not consider the presence of water in the structure, in contrast to the standard model. Thus, the new ferrihydrite model violates Pauling's 2nd rule for ionic structures, which states that the sum of the bond valences around each atom or functional group in a structure should equal its oxidation state, here 3+ for Fe and 1− for OH (Pauling, 1929, 1960).

The new model is also unrealistic from a coordination-chemistry perspective because it defies basic principles of crystal chemistry: it has (1) a tetrahedral site larger than (Fhyd2, Fhyd3), or similar in size (Fhyd6) to, an octahedral site; (2) a tetrahedral site more distorted than an octahedral site (Fhyd3, Fhyd6); (3) a mean octahedral ^{VI}Fe−O distance as short as 1.92 Å (Fhyd3, Fhyd6); and (4)

three sites, one tetrahedral and two octahedral (Fhyd2), of approximately the same dimension (1.98 and 2×2.00 Å) (Tables 3, 4, and 5). As a comparison, a survey of 204 Fe−O binding environments in the Inorganic Crystal Structure Database shows that $<d(^{VI}Fe^{3+}-O)>$ = 2.015 Å and $<d(^{IV}Fe^{3+}-O)>$ = 1.865 Å (Brown & Altermatt, 1985).

CONCLUSION

It is important to emphasize that the standard ferrihydrite model (Drits *et al.*, 1993a) has been buttressed by single-crystal electron nanodiffraction (Janney *et al.*, 2001). When the dimensions of a crystal are large enough for characterization by single-crystal diffraction, this technique is arguably more robust than the PDF method because it gives a 3-D and not a 2-D representation of its 3-D structure. Beam-induced structural changes under high vacuum and focused electron beam in the studies by Janney *et al.* (2000, 2001) and Cowley *et al.* (2000) are unlikely, otherwise their results would not be consistent with XRD data at ambient conditions. Therefore, ferrihydrite is definitely not monophasic but consists of variable mixtures of related phases of different crystallinity which depend on the synthesis conditions. The polyphasic and defective nature of ferrihydrite can no longer be ignored in future structural studies.

ACKNOWLEDGMENTS

Advanced Light Source (Berkeley, California) is supported by the Director, Office of Energy Research, Office of Basic Energy Sciences, Materials Sciences Division of the U.S. Department of Energy, under Contract No. DE-AC02-05CH11231.

REFERENCES

Ankudinov A.L., Ravel B., Rehr J.J. & Conradson S.D. (1998) Real space multiple scattering calculation of XANES. *Physical Review*, **B58**, 7565−7576.

Bino A., Ardon M., Lee D., Spingler B. & Lippard S.J. (2002) Synthesis and structure of $[Fe_{13}O_4F_{24}(OMe)_{12}]^{5-}$: The first open-shell Keggin ion. *Journal of the American Chemical Society*, **124**, 4578−4579.

Blake R.L., Hessevick R.E., Zoltai T. & L.F. (1966) Refinement of the hematite structure. *American Mineralogist*, **51**, 123−129.

Bradley M. & Kydd R.A. (1993) Comparison of the species formed upon base hydrolyses of gallium(III) and iron(III) aqueous solutions: The possibility of existence of an $[FeO_4Fe_{12}(OH)_{24}(H_2O)_{12}]^{7+}$ polyoxocation. *Journal of the Chemical Society, Dalton Transactions*, 2407−2413.

Bradley S.M., Kydd R.A. & Fyfe C.A. (1992) Characterization of the $GaAl_{12}(OH)_{24}(H_2O)_{12}^{7+}$ polyoxocation by MAS NMR and infrared spectroscopies and powder X-ray diffraction. *Inorganic Chemistry*, **31**, 1181−1185.

Brown I.D. (1976) On the geometry of O-H....O hydrogen bonds. *Acta Crystallographica*, **A32**, 24−31.

Brown I.D. (1992) Chemical and steric constraints in inorganic solids. *Acta Crystallographica*, **B48**, 553−572.

Brown I.D. & Altermatt D. (1985) Bond-valence parameters obtained from a systematic analysis of the Inorganic Crystal Structure Database. *Acta Crystallographica*, **B41**, 244−247.

Catalano J.G., Park C., Zhang Z. & Fenter P. (2006) Termination and water adsorption at the α-Al_2O_3 (012) − aqueous solution interface. *Langmuir*, **22**, 4668−4673.

Combes J.M., Manceau A. & Calas G. (1990) Formation of ferric oxides from aqueous solutions: a polyhedral approach by X-ray absorption spectroscopy. II. Hematite formation from ferric gels. *Geochimica et Cosmochimica Acta*, **54**, 1083−1091.

Cowley J.M., Janney D.E., Gerkin R.C. & Buseck P.R. (2000) The structure of ferritin cores determined by electron nanodiffraction. *Journal of Structural Biology*, **131**, 210−216.

De Grave E., Vandenberghe R.E. & Dauwe C. (2005) ILEEMS: Methodology and applications to iron oxides. *Hyperfine Interactions*, **161**, 147−160.

Drits V.A., Sakharov B.A., Salyn A.L. & Manceau A. (1993a) Structural model for ferrihydrite. *Clay Minerals*, **28**, 185−208.

Drits V.A., Sakharov B.A. & Manceau A. (1993b) Structure of feroxyhite as determined by simulation of X-ray diffraction curves. *Clay Minerals*, **28**, 209−222.

Drits V.A., Gorshkov A.I., Sakharov B.A., Salyn A.L. & Manceau A. (1995) Ferrihydrite and its phase transitions during heating in the oxidizing and reducing environments. *Lithology and Mineral Resources* (translated from *Litologiya*, **1**, 76-84, 1995), **1**, 68−75.

Eggleton R.A. & Fitzpatrick R.W. (1988) New data and a revised structural model for ferrihydrite. *Clays and Clay Minerals*, **36**, 111−124.

Hawthorne F.C. (1994) Structural aspects of oxide and oxysalt crystals. *Acta Crystallographica*, **B50**, 481−510.

Hazemann J.L., Bérar J.F. & Manceau A. (1991) Rietveld studies of the aluminium-iron substitution

in synthetic goethite. *Materials Sciences Forum*, **79-82**, 821–826.

Hwang S.L., Shen P.Y., Chu H.T. & Yui T.F. (2006) A new occurrence and new data on akdalaite, a retrograde mineral from UHP Whiteschist, Kokchetav Massif, Northern Kazakhstan. *International Geology Review*, **48**, 754–764.

Janney D.E., Cowley J.M. & Buseck P.R. (2000) Structure of synthetic 2-line ferrihydrite by electron nanodiffraction. *American Mineralogist*, **85**, 1180–1187.

Janney D.E., Cowley J.M. & Buseck P.R. (2001) Structure of synthetic 6-line ferrihydrite by electron nanodiffraction. *American Mineralogist*, **86**, 327–335.

Jansen E., Kyek A., Schafer W. & Schwertmann U. (2002) The structure of six-line ferrihydrite. *Applied Physics A – Materials Science & Processing*, **74**, S1004–S1006.

Jolivet J.P. (2000) *Metal Oxide Chemistry and Synthesis: From Solution to Solid State*. Wiley, New York.

Li M.X., Jin S.L., Liu H.Z., Xie G.Y., Chen M.Q., Xu Z. & You X.Z. (1998) A novel hydroxo-bridged ferric bisubstituted Keggin heteropolytungstate dimer: synthesis and crystal structure of $(Me_4N)_{10}[Fe_4(OH)_4(PW_{10}O_{37})_2].15H_2O$. *Polyhedron*, **17**, 3721–3725.

Lo C.S., Kunaljeet S., Tanwar S., Chaka A.M. & Trainor T.P. (2007) Density functional theory study of the clean and hydrated hematite surfaces. *Physical Review*, **B75**, 075425.

Manceau A. & Combes J.M. (1988) Structure of Mn and Fe oxides and oxyhydroxides: a topological approach by EXAFS. *Physics and Chemistry of Minerals*, **15**, 283–295.

Manceau A. & Drits V.A. (1993) Local structure of ferrihydrite and feroxyhite by EXAFS spectroscopy. *Clay Minerals*, **28**, 165–184.

Manceau A. & Gates W. (1997) Surface structural model for ferrihydrite. *Clays and Clay Minerals*, **43**, 448–460.

Manceau A., Combes J.M. & Calas G. (1990) New data and a revised model for ferrihydrite: a comment on a paper by R. A. Eggleton and R. W. Fitzpatrick. *Clays and Clay Minerals*, **38**, 331–334.

Manceau A., Chateigner D. & Gates W.P. (1998) Polarized EXAFS, distance-valence least-squares modeling (DVLS) and quantitative texture analysis approaches to the structural refinement of Garfield nontronite. *Physics and Chemistry of Minerals*, **25**, 347–365.

Manceau A., Marcus M.A. & Tamura N. (2002) Quantitative speciation of heavy metals in soils and sediments by synchrotron X-ray techniques Pp. 341–428 in: *Applications of Synchrotron Radiation in Low-Temperature Geochemistry and Environmental Science* (P.A. Fenter, M.L. Rivers, N.C. Sturchio & S.R. Sutton, editors). Mineralogical Society of America, Washington, D.C.

Marcus M.A., MacDowell A.A., Celestre R., Manceau A., Miller T., Padmore H.A. & Sublett R.E. (2004) Beamline 10.3.2 at ALS: a hard X-ray microprobe for environmental and materials sciences. *Journal of Synchrotron Radiation*, **11**, 239–247.

Michel F.M., Ehm L., Antao S.M., Lee P.L., Chupas P.J., Liu G., Strongin D.R., Schoonen M.A.A., Phillips B.L. & Parise J.B. (2007a) The structure of ferrihydrite, a nanocrystalline material. *Science*, **316**, 1726–1729.

Michel F.M., Ehm L., Liu G., Han W., Antao S.M., Chupas P.J., Lee P.L., Knorr K., Eulert H., Kim J., Grey C.P., Celestian A.J., Gillow J., Schoonen M.A.A., Strongin D. & Parise J.B. (2007b) Similarities in structure of coherent scattering domains in 2- and 6-line ferrihydrite and effect of particle size. *Chemistry of Materials*, **19**, 1489–1496.

Pankhurst G.A. & Pollard R.J. (1992) Structural and magnetic properties of ferrihydrite. *Clays and Clay Minerals*, **40**, 268–272.

Patrat G., De Bergevin F., Pernet M. & Jourbert J.C. (1983) Structure locale de δFeOOH. *Acta Crystallographica*, **B39**, 165–170.

Pauling L. (1929) The principles determining the structure of complex ionic crystals. *Journal of the American Chemical Society*, **51**, 1010–1026.

Pauling L. (1960) *The Nature of the Chemical Bond*. Cornell University Press, Ithaca, New York.

Rowsell J. & Nazar F. (2000) Speciation and thermal transformation in alumina sols: Structures of the polyhydroxyoxoaluminum cluster $[Al_{30}O_8(OH)_{56}(H_2O)_{26}]^{18+}$ and its δ-Keggin moité. *Journal of the American Chemical Society*, **122**, 3777–3778.

Schwertmann U., Friedl J. & Stanjek H. (1999) From Fe(III) ions to ferrihydrite and then to hematite. *Journal of Colloid and Interface Science*, **209**, 215–223.

Stern E.A. & Kim K. (1981) Thickness effect on the extended-X-ray-absorption-fine-structure amplitude. *Physical Review*, **B23**, 3781–3787.

Tanwar K.S., Lo C.S., Eng P.J., Catalano J.G., Walko D.A., Brown G.E.J., Waychunas G.A., Chaka A.M. & Trainor T.P. (2007) Surface diffraction study of the hydrated hematite surface. *Surface Science*, **601**, 460–474.

Towe K.M. & Bradley W.F.J. (1967) Mineralogical constitution of colloid 'hydrous ferric oxides'. *Journal of Colloid and Interface Science*, **24**, 384.

Waychunas G.A., Fuller C.C., Rea B.A. & Davis J.A. (1996) Wide angle X-ray scattering (WAXS) study of ''two-line'' ferrihydrite structure: Effect of arsenate sorption and counterion variation and comparison with EXAFS results. *Geochimica et*

Cosmochimica Acta, **60**, 1765–1781.

Yamaguchi G. & Okumiya M. (1969) Refinement of the structure of tohdite $5Al_2O_3.H_2O$. *Bulletin of the Chemical Society of Japan*, **42**, 2247–2249.

Yamaguchi G., Okumiya M. & Ono S. (1964) The crystal structure of tohdite. *Bulletin of the Chemical Society of Japan*, **37**, 1555–1557.